MINISTÉRIO DA EDUCAÇÃO

UNIVERSIDADE FEDERAL DO TRIÂNGULO MINEIRO

PROGRAMA DE PÓS-GRADUAÇÃO EM CIÊNCIAS FISIOLÓGICAS

Amanda Damasceno Brasileiro

Efeitos da diabetes mellitus na densidade neuronal mioentérica e na expressão de canais de sódio no íleo de ratas.

Uberaba - MG

2018

AMANDA DAMASCENO BRASILEIRO

Efeitos da diabetes mellitus na densidade neuronal mioentérica e na expressão de canais de sódio no íleo de ratas.

Dissertação apresentada ao Programa de Pós-Graduação em Ciências Fisiológicas, área de concentração I: Bioquímica, Fisiologia e Farmacologia, da Universidade Federal do Triângulo Mineiro, como requisito parcial para obtenção do título de mestra em Ciências Fisiológicas.

Orientador: Prof. Dr. Aldo Rogelis Aquiles Rodrigues.

Uberaba-MG

2018

AMANDA DAMASCENO BRASILEIRO

Efeitos da diabetes mellitus na densidade neuronal mioentérica e na expressão de canais de sódio no íleo de ratas.

Dissertação apresentada ao Programa de Pós-Graduação em Ciências Fisiológicas, área de concentração I: Bioquímica, Fisiologia e Farmacologia, da Universidade Federal do Triângulo Mineiro, como requisito parcial para obtenção do título de mestra em Ciências Fisiológicas.

Aprovado em: ___ de _____ de _____.

BANCA EXAMINADORA

_____

Prof. Dr. Aldo Rogelis Aquiles Rodrigues – Orientador

Universidade Federal do Triângulo Mineiro (UFTM)

_____

Prof. Dr. André Schwambach Vieira

Universidade Estadual de Campinas (Unicamp)

_____

Profa. Dra. Maria Emília Soares Martins dos Santos

Universidade Federal do Triângulo Mineiro (UFTM)

DEDICATÓRIA

Este trabalho, bem como todo esforço e paciência nele contidos, é dedicado aos meus pais e irmãos, ao meu namorado e a todos os meus amigos. Também àqueles que, de alguma forma, contribuíram para a concretização desse sonho.

AGRADECIMENTOS

Acima de tudo e de todos, gratidão a Deus. Porque Dele, por Ele e para Ele são todas as coisas.

Gratidão aos meus pais, Kelma e Renan, por toda dedicação, zelo, paciência, esforço e por se desdobrarem em milhões para que esse ciclo se finalizasse. Aos meus irmãos José Neto e Arthur pelo apoio de sempre. Não há palavras para agradecer o suficiente. Vocês são o elo de amor que me sustenta e motiva. O amor de vocês é o maior presente que já recebi na vida. Essa conquista é para vocês. Eu amo vocês!

Ao meu namorado, Janir Filho. Por toda sua paciência, seu ombro amigo, suas palavras de ânimo e conforto e por todo seu amor. Você fez dessa caminhada mais leve e se fez apoio quando me senti cansada. Com você eu sei que posso ir mais longe. Obrigada por tudo. Eu amo você!

Aos meus amigos, os verdadeiros, que sempre torceram por mim e que se alegram com essa conquista, o meu muito obrigada. Especialmente ao Mestre Eduardo Henrique Tavares (Dudu), companheiro de faculdade, de mestrado e um irmão sempre que precisei nesses anos em Uberaba. Aos amigos que a UFTM e Uberaba me deram, gratidão eterna.

Ao meu orientador Doutor Aldo Rogelis Aquiles Rodrigues, por toda paciência e dedicação. Poucas pessoas têm a chance de ter um orientador com tanta boa vontade e disposição, com tanto empenho para fazer dar certo. Mais que um orientador, um amigo. Estendendo meu agradecimento também à sua esposa Lucieny Almohalha, por sua hospitalidade e generosidade. Aos dois, obrigada por tudo!

Aos meus colegas do PPGCF, companheiros de caminhadas e de dificuldades nesse processo chamado pós-graduação. Gratidão e votos de sucesso a todos.

Aos professores do programa, os quais souberam tão generosamente dividir seus conhecimentos. Aos técnicos dos laboratórios da UFTM que sempre dispostos me auxiliaram e ensinaram.

À secretária do PPGCF, Elisabete Perez Caramori Ambrosio, por não medir esforços para me atender e estar sempre disposta com um lindo sorriso para me ajudar. Você é luz. Eterna gratidão a você.

Por último, porém com importância extrema, à Fundação de Amparo à Pesquisa do Estado de Minas Gerais (FAPEMIG) pelo apoio financeiro para que eu pudesse ter condições de realizar todas as minhas atividades na pós-graduação para o desenvolvimento deste trabalho. Lembrando, ainda, de sua importância para a ciência no âmbito nacional.

“Não te mandei eu? Esforça-te, e tem bom ânimo; não temas, nem te espantes; porque o Senhor teu Deus é contigo, por onde quer que andares.”

Josué 1:9

RESUMO

A diabetes mellitus (DM) pode levar a distúrbios da motilidade gastrointestinal que podem se tornar clinicamente relevantes em alguns pacientes. Modelos de Dm em roedores indicam anormalidades morfofuncionais do sistema nervoso entérico nessa doença. Neste trabalho, avaliamos se o DM experimental pode levar a alterações na eferência colinérgica excitatória, densidade neuronal e expressão dos canais de sódio voltagem-dependente (Nav) no plexo mioentérico do íleo. Hiperglicemia induzida por estreptozotocina em ratas foi desenvolvida durante oito semanas. Experimentos de imunofluorescência de tripla marcação revelaram que a densidade de neurônios por área do íleo no DM foi significativamente reduzida quando comparada ao controle. Foram observadas reduções médias de 52,2% do total de neurônios (p=0,0001); 50,0% dos neurônios colinérgicos (p=0,0068) e 54,8% dos neurônios nitrérgicos (p=0,0042). Também foram observadas reduções significativas de neurônios por área de gânglio (28,2% do total, p=0,0002; 27,7% de colinérgicos, p= 0,0002 e 32,1% de neurônios nitrérgicos, p=0,0016). A densidade de fibras colinérgicas na superfície do músculo longitudinal também foi significativamente reduzida (controle: 41 ± 2, DM: 24 ± 3%; p=0,003), embora a análise western-blot não indicasse redução na expressão de ChAT no DM. grupo. A isoforma Nav1.6 foi detectada em diferentes neurônios mioentéricos e a DM tendeu a mudar o padrão de imunomarcação para neurônios de tamanho maior (297,4 ± 10 vs. 372,5 ± 8,4 μm^2), mas esse efeito não foi significativo (p=0,3). Os dados de RT-qPCR não sugeriram uma alteração dos transcritos para ChAT, nNOS, Nav1.3, Nav1.6 ou Nav1.7. Nossos dados confirmam a visão de que o DM crônico leva à redução das fibras colinérgicas excitatórias e da densidade neuronal. No entanto, mudanças no perfil de expressão do canal de sódio, que poderiam levar à disfunção neuronal, não foram detectadas.

Palavras-chave: Diabetes mellitus; Sistema nervoso entérico; Canais de sódio; Disfunções gastrointestinais; Neurônios colinérgicos; Neurônios nitrérgicos.

ABSTRACT

Diabetes mellitus (DM) may lead to gastrointestinal motility disorders that may become clinically relevant in some patients. Rodent models of DM indicate morpho-functional abnormalities of the enteric nervous system in this disease. In this work, we have evaluated whether experimental DM can lead to changes in excitatory cholinergic efference, neuronal density and voltage-gate sodium channels (Nav) expression in the myenteric plexus of ileum. Streptozotocin-induced hiperglycemia in female rats was allowed to develop during eight weeks. Triple immunofluorescence labeling experiments revealed that the density of neurons per area of ileum in DM was significantly reduced when compared to the control. It were observed average reductions of 52.2% of total neurons (p=0.0001); 50.0% of cholinergic (p=0.0068) and 54.8% of nitrergic neurons (p=0.0042). Significant reductions of neurons per area of ganglion were also observed (28.2% of total, p=0.0002; 27.7% of cholinergic, p=0,0002 and 32.1% of nitrergic neurons, p=0.0016). The cholinergic fibers density at the surface of longitudinal muscle was also significantly reduced (control: 41 ± 2, DM: 24 ± 3%; p=0.003), although western-blot analysis did not indicate a reduction in the expression of ChAT in DM group. The Nav1.6 isoform was detected in different myenteric neurons and DM tended to shift the immunolabeling pattern towards neurons of bigger size (297.4 ± 10 vs. 372.5 ± 8.4 μm^2), but this effect was not significant (p=0.3). RT-qPCR data did not suggest an alteration of transcripts for ChAT, nNOS, Nav1.3, Nav1.6 or Nav1.7. Our data support the view that chronic DM leads to reduction in excitatory cholinergic fibers and neuronal density. However, changes in sodium channel expression profiling, which could lead to neuronal dysfunction, were not detected.

Keywords: Diabetes mellitus; Enteric nervous system; Sodium channels; Gastrointestinal disorders; Cholinergic neurons; Nitrergic neurons.

SUMÁRIO

1 REVISÃO

1.1 O SISTEMA NERVOSO ENTÉRICO E DIABETES MELLITUS

O sistema nervoso entérico (SNE) se estende da parede esofágica até o esfíncter anal e é a maior e mais complexa divisão do sistema nervoso periférico autonômico em vertebrados (Figura 1). Semelhante ao observado no sistema nervoso central (SNC), o SNE contém numerosos e variados tipos de neurônios, neurotransmissores e neuromoduladores (Furness, 2012). O SNE é composto de aproximadamente cem milhões de neurônios entéricos e de células gliais que se organizam em dois grandes plexos: plexo mioentérico e submucoso (Uesaka et al., 2016). Essa rede interconectada controla a motilidade e secreção gastrointestinal, a troca de fluidos na superfície da mucosa, o fluxo sanguíneo e a secreção de hormônios no intestino (Brookes e Costa, 2006).

Figura 1 - Esboço do sistema nervoso entérico.

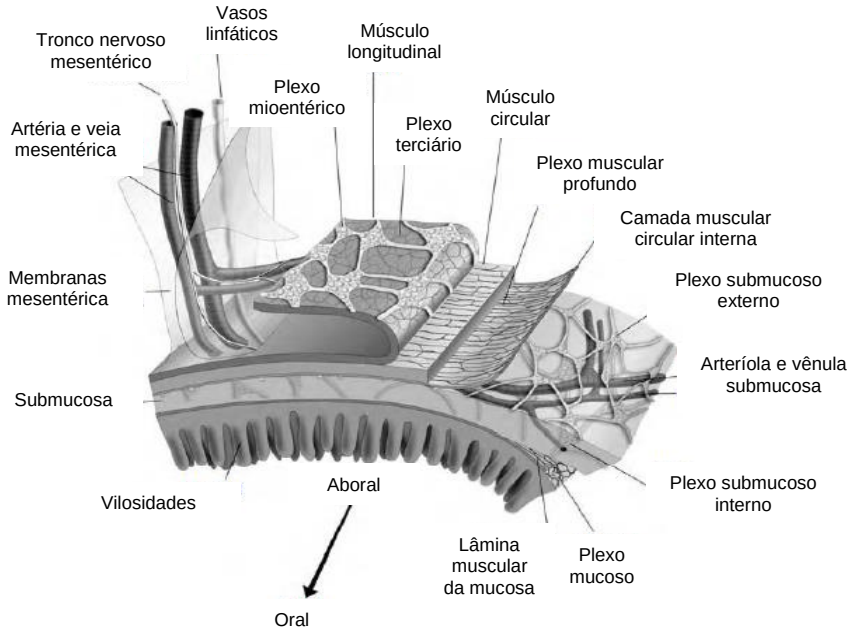

Representação dos plexos mioentérico e submucoso na parede do TGI. Fonte: BROOKES e COSTA, 2006.

Pelo fato de o SNE ser tão diferente de outros gânglios autonômicos, ele possui mecanismos capazes de codificar a expressão da diversidade fenotípica neuronal entérica, o desenvolvimento de microcircuitos intrínsecos e o estabelecimento de sinapses. Tais circuitos são capazes de integrar informações sobre as condições luminais

ou da parede do intestino que são percebidas por neurônios sensoriais locais (aferência intrínseca), gerando respostas locais (Brookes e Costa, 2006). Dessa forma, mecanismos intrínsecos intestinais são capazes de gerar respostas locais por meio dos reflexos secreto-motores (Furness, 2012). Entretanto, sabe-se que a atividade dos neurônios entéricos é bastante modulada pelo sistema nervoso autonômico simpático e parassimpático (Uesaka et al., 2016).

A inervação parassimpática é feita pelo nervo vago (X par craniano) que inerva esôfago, estômago, intestino delgado e parte proximal do intestino grosso. O nervo vago promove uma comunicação bilateral entre o SNC e o SNE, tendo o SNC uma poderosa habilidade de inibir ou excitar o SNE, e o SNE tem uma capacidade notável de perturbar o SNC. A inervação simpática é feita pelos gânglios celíaco, mesentérico superior, mesentérico inferior e hipogástrico (Furness, 2012).

No SNE foram encontradas várias classes de neurônios, dentre elas: neurônios sensoriais intrínsecos primários (IPANs), interneurônios e neurônios excitatórios e inibitórios que inervam células efetoras da parede do TGI (Furness, 2012). O plexo mioentérico (PM) está localizado entre a camada muscular circular e a longitudinal e se estende por todo o comprimento da parede intestinal e como se localiza entre as camadas musculares, está mais envolvido no controle da atividade muscular no TGI. Quando o plexo mioentérico é estimulado ocorre aumento do tônus na parede intestinal, da intensidade das contrações rítmicas, do ritmo das contrações e na velocidade de condução das ondas excitatórias ao longo da parede intestinal causando um aumento no peristaltismo. Porém o plexo mioentérico não é totalmente excitatório, pois possui neurônios que produzem em suas fibras neurotransmissores inibitórios (Guyton e Hall, 2011). Esses neurônios motores excitatórios e inibitórios da musculatura longitudinal do SNE têm como neurotransmissores primários a acetilcolina (ACh) e o óxido nítrico (NO), respectivamente. Os neurotransmissores excitatórios são responsáveis por mediar a contração da musculatura lisa em toda região intestinal (Furness, 2000), enquanto os inibitórios são liberados por fibras não-adrenérgicas e não-colinérgicas (Brehmer, Schrold e Neuhuber, 2006; De Giorgio et al., 1994). Sabe-se que a acetilcolina é sintetizada pela enzima colina acetiltransferase (ChAT), a qual é considerada um indicador do estado funcional de neurônios colinérgicos no sistema nervoso central e periférico (Oda, 1999), além de ser o neurotransmissor mais encontrado no SNE (Nakajima et al., 2000). O óxido

nítrico, por sua vez, é sintetizado pela óxido nítrico sintase neuronal (nNOS) e é considerado o principal neurotransmissor inibitório no SNE (Surendran e Kondopaka, 2005).

Ainda, em relação à inervação intrínseca do TGI, observa-se no SNE as células intersticiais de Cajal (ICCs) que são células presentes em muitas camadas da parede do TGI e que apresentam morfologia e função diferentes de acordo com sua localização. As ICC apresentam uma função de marca-passo, gerando atividade elétrica que resulta em um movimento peristáltico de ondas lentas em várias partes do TGI (Sanders, Koh e Helke, 2006; Thuneberg, 1987). Além de estarem envolvidas na neurotransmissão entre neurônios motores, eferências do SNC e células do músculo liso da parede do TGI (Ward et al., 2000; Ward, McLaren e Sanders, 2006).

Sabe-se que a Diabetes Mellitus (DM) é uma síndrome caracterizada por hiperglicemia crônica e degenerativa causada por anormalidades no metabolismo de carboidratos, proteínas e gorduras devido à deficiência na secreção de insulina e/ou redução do seu efeito biológico, estando associada a disfunção e danos em vários tecidos e sistemas (Rodrigues e Motta, 2012). Os dados mais recentes da International Diabetes Federation (IDF) indicaram que a DM afetou 382 milhões de pessoas em todo o mundo em 2013, número que deverá crescer para 592 milhões até 2035, caracterizando a DM como um problema de saúde pública mundial (Seuring, Archangelidi e Suhrcke, 2015). A DM se manifesta com sintomas gastrointestinais, sendo eles: vômitos, náuseas, diarreia, constipação, dor abdominal, disfagia e incontinência fecal (Rodrigues e Motta, 2012). Esses sintomas gastrointestinais são declaradamente comuns na clínica médica em paciente com DM. Em um estudo realizado por Folwaczny et al. (1999), 75% dos pacientes relataram sintomas gastrointestinais significativos, os quais eram mais frequentes naqueles com um controle glicêmico inadequado. Todo o TGI, do esôfago até a região anorretal, pode ser afetado com diferentes manifestações e distúrbios sensório-motores. Em muitos casos, esses sintomas são correlacionados às anormalidades na motilidade gastrointestinal que, por sua vez, pode ser uma manifestação da neuropatia autonômica diabética que acomete o TGI.

A patogenia destas desordens na diabetes é complexa, multifatorial (neuropatia autonômica, deficiente controle glicêmico, fatores psicológicos) e ainda necessita de avanços para ser mais bem compreendida (Horowitz et al., 2004). Nos últimos anos, o

papel do SNE e seus neurotransmissores tem ganhado significância nas manifestações gastrointestinais dessa patologia endócrina (Yarandi e Srinivasan, 2014; Kamenov e Traykov, 2012); porém em contraste com as disfunções gástricas, as deficiências funcionais oriundas de alterações provocadas pela DM no intestino delgado e grosso foram menos intensamente estudadas, apesar de sua notável clínica nesses pacientes (Horváth et al., 2015).

Em pacientes com DM, as fibras do nervo vago apresentam desmielinização e degeneração axonal tanto fora do TGI quanto ao nível do plexo mioentérico e submucoso levando à neuropatia entérica (Guy et al., 1984; Smith, 1974). Há que se observar também que as fibras aferentes vagais estão muito correlacionadas com as células ICC e a expressão de nNOS que também contribuem para os sintomas no TGI (Regalia, Cai e Helke, 2002). Além disso, podemos citar a remodelação histomorfológica induzida pelo descontrole glicêmico, neste caso a hiperglicemia, que também pode desempenhar um papel importante no desenvolvimento das anormalidades sensório-motoras do TGI (Zhao et al., 2010). Nesse sentido, em relação à densidade neuronal, os efeitos da DM na população de neurônios entéricos têm sido estudados em modelos com uso de diabetes induzida por estrepzotocina em ratos, e essa diminuição tem sido observada no estômago (Fregonesi et al., 2001), íleo (Alves et al., 2006), ceco (Zanoni et al., 1997) e cólon (Du et al., 2009), ressaltando a diminuição da população de neurônios colinérgicos e, possivelmente, diminuição da eferência colinérgica.

Assim, torna-se necessário o melhor entendimento dos mecanismos que envolvem as suas manifestações, já que se trata de uma patologia de grande prevalência e importante impacto na saúde pública mundial. Compreender os mecanismos dessas desordens no TGI é fundamental para aperfeiçoar o tratamento e para encontrar novas abordagens terapêuticas, a fim de proporcionar melhor qualidade de vida a esses pacientes.

1.2 CANAIS DE SÓDIO VOLTAGEM DEPENDENTE

Os canais de sódio voltagem-dependentes (Nav) estão envolvidos com a iniciação e propagação dos potenciais de ação em neurônios, células musculares e alguns tipos de células neuroendócrinas. Quando a membrana é despolarizada os canais Nav se ativam e inativam em milissegundos permitindo um influxo rápido e transitório de íons sódio e iniciando o potencial de ação. Existem nove subtipos de canais Nav, denominados

Nav1.1 a Nav1.9, que foram encontrados distribuídos heterogeneamente em tecidos de mamíferos (Caterall, Goldin e Waxman, 2005).

Figura 2 - Provável organização dos canais de sódio voltagem-dependentes na membrana plasmática celular.

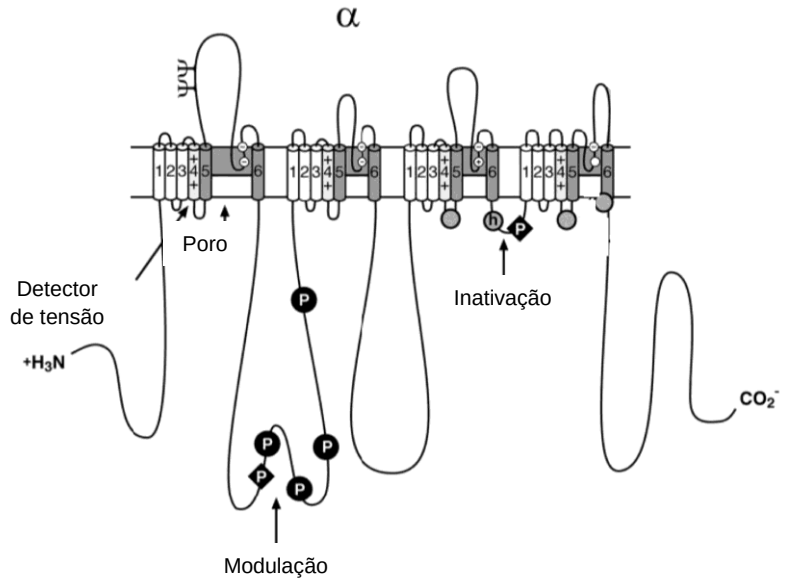

Linha representa a sequência polipeptídica cujo tamanho reflete o número de aminoácidos e os cilindros prováveis segmentos transmembrana. Sítios de fosforilação (P) são indicados bem como sítios de N-glicosilação (Ψ), os sensores de voltagem de cada domínio são indicados por ++ (resíduos de carga positiva), a partícula de inativação é representada por h, sequência entre os segmentos transmembrana S5 e S6 de cada domínio contribuem para formação do poro iônico do canal. Fonte: modificado de CATTERALL, GOLDIN e WAXMAN, 2005.

Os canais Nav desempenham importante papel na atividade elétrica dos neurônios entéricos do TGI. No SNE do íleo e cólon de cobaias, os transcritos para as isoformas Nav1.2, 1.3, 1.6 e 1.7 foram detectadas por Bartoo, Sprunger e Schneider (2005). Esses autores detectaram por imunorreatividade Nav1.2 no soma; Nav1.3 em dendritos, soma e fibras que interconectam os gânglios do plexo mioentérico e Nav1.6 no segmento inicial de axônios. Os canais Nav1.6 foram observados somente em neurônios do cólon e não no plexo mioentérico do intestino delgado. Já em outro estudo Sage et al. (2007), usando diferentes técnicas moleculares, demonstraram a expressão de Nav1.3 e também de 1.7 em neurônios do plexo mioentérico duodenal de cobaias, apesar de as isoformas Nav1.7 e também 1.6 não terem sido detectadas por imunohistoquímica.

Em neurônios do gânglio da raíz dorsal (DRG), Nav1.3 é expressa em estágios iniciais do desenvolvimento neuronal e não é observada em ratos adultos. Interessantemente, esses canais são expressos novamente após axotomia periférica (Waxman, Kocsis e Black, 1994). Outros estudos têm mostrado que a expressão de Nav1.3 é suprarregulada em neurônios do DRG em casos de danos nervosos (Black et al., 1999) e também na dor neuropática associada com DM (Craner et al., 2002; Tan et al., 2015). Há evidências que essa neuropatia diabética possa levar ao aumento da expressão de Nav1.6 em neurônios do DRG (Craner et al., 2002) ou redução (Hong et al., 2004) enquanto Nav1.7 parece aumentar na doença (Huang et al., 2014). Embora seja possível associar mudanças na expressão de canais de sódio à neuropatia diabética em neurônios do DRG, não foram encontrados estudos que avaliaram a expressão de canais de sódio voltagem-dependentes durante o curso da diabetes crônica em neurônios entéricos.

As isoformas Nav1.3, Nav1.6 e Nav1.7, alvos do presente estudo, estão incluídas entre os canais de sódio tetrodotoxina sensíveis. O canal Nav1.3 quando expresso em células HEK293 exibe uma cinética rápida de ativação e inativação e a recuperação da inativação é rápida em potenciais negativos (-80 mV) e lenta em potenciais mais positivos. Esses canais exibem também uma lenta inativação a partir do estado fechado, de modo que, neurônios que o expressam, podem gerar potenciais de ação quando o estímulo despolarizante é mais lento, contribuindo para a excitabilidade neuronal, além de permitir o disparo de potenciais de ação repetidos em frequências mais altas (Cummins et al., 2001). Os canais Nav1.6 produzem uma corrente de rápida ativação e que se inativa parcialmente gerando uma corrente persistente que contribui para aumento da excitabilidade neuronal. Além dessa corrente persistente foi observada em algumas células a geração de uma corrente ressurgente após repolarizações parciais, indicando que os canais podem não transitar para o estado de inativação clássico (inativação por domínio N-terminal do canal), o que também poderia contribuir para disparos de potenciais de ação repetidos em alta frequência (Chen et al., 2008; Enomoto et al., 2018). A isoforma Nav1.7, apresenta uma lenta cinética de inativação a partir do estado fechado, desempenhando um papel importante na amplificação de despolarizações sublimiares e iniciação do potencial de ação em neurônios (Blair e Bean, 2002; Cummins, Sheets e Waxman, 2007).

REFERÊNCIAS

Alves AM, Alves EP, Fregonesi CET, Defani MA, Stabille SR, Evangelista CC, dos Santos CA, Miranda-Neto MH. Morphoquantitative aspects of NADH-diaphorase myenteric neurons in the ileum of diabetic rats treated with acetyl-L-carnitine. Anat Histol Embryol. 2006 Feb;35(1):13-8.

Bartoo AC, Sprunger LK, Schneider DA. Expression and distribution of TTX Sensitive Sodium Channel Alpha Subunits in the Enteric Nervous System. J Comp Neurol. 2005 May 30;486(2):117-31.

Black JA, Cummins TR, Plumpton C, Chen YH, Hormuzdiar W, Clare JJ et al. Upregulation of a silent sodium channel after peripheral, but not central, nerve injury in DRG neurons. J Neurophysiol. 1999 Nov;82(5):2776-85.

Blair NT, Bean BP. Roles of tetrodotoxin (TTX)-sensitive Na^+ current, TTX-resistant Na^+ current, and Ca^{2+} current in the action potentials of nociceptive sensory neurons. J Neurosci. 2002 Dec 1;22(23):10277-90.

Brehmer A, Schrodl F, Neuhuber W. Morphology of VIP/nNOS-immunoreactive myenteric neurons in the human gut. Histochem Cell Biol. 2006 May;125(5):557-65.

Brookes SJH, Costa M. Functional Histoanatomy of the Enteric Nervous System. In: Johnson LR. Physiology of the Gastrointestinal Tract. 4 ed. London: United Kingdom, 2006. Cap. 21, p. 577-602.

Caterall WA, Goldin AL, Waxman SG. International union of pharmacology. XLVII. Nomenclature and structure-function relationships of voltage-gated sodium channels. Pharmacol Rev. 2005 Dec;57(4):397-409.

Craner MJ, Klein JP, Renganathan M, Black JA, Waxman SG: Changes of sodium channel expression in experimental diabetic neuropathy. Ann Neurol. 2002 Dec;52(6):786-92.

Cummins TR, Aglieco F, Renganathan M, Herzog RI, Dib- Hagg SD, Waxman SG. Nav1.3 sodium channels: rapid repriming and slow closed-state inactivation display quantitative differences after expression in a mammalian cell line and in spinal sensory neurons. J Neurosci. 2001 Aug 15;21(16):5952-61.

Cummins TR, Sheets PL, Waxman SG. The roles of sodium channels in nociception: Implications for mechanisms of pain. Pain. 2007 Oct;131(3):243-57.

De Giorgio R, Parodi JE, Brecha NC, Brunicardi FC, Becker JM, Go VL, Sternini C. Nitric oxide producing neurons in the monkey and human digestive system. J Comp Neurol. 1994 Apr 22;342(4):619-27.

Du F, Wang L, Qian W, Liu S. Loss of enteric neurons accompanied by decreased expression of GDNF and PI3K/Akt pathway in diabetic rats. Neurogastroenterol Motil. 2009 Nov;21(11):1229-e114.

Enomoto A, Seki S, Tanaka S, Ishihama K, Yamanishi T, Kogo M et al. Development of resurgent and persistent sodium currents in mesencephalic trigeminal neurons. J Neurosci Res. 2018 Feb;96(2):305-312.

Folwaczny C, Riepl R, Tschöp M, Landgraf R. Gastrointestinal involvement in patients with diabetes mellitus: Part I (first of two parts). Epidemiology, pathophysiology, clinical findings. Z Gastroenterol. 1999 Sep;37(9):803-15.

Fregonesi CE, Miranda-Neto MH, Molinari SL, Zanoni JN. Quantitative study of the myenteric plexus of the stomach of rats with streptozotocin-induced diabetes. Arq Neuropsiquiatr. 2001 Mar;59(1):50-3.

Furness JB. Types of neurons in the enteric nervous system. J Auton Nerv Syst. 2000 Jul 3;81(1-3):87-96.

Furness JB. The enteric nervous system and neurogastroenterology. Nat Rev Gastroenterol Hepatol. 2012 Mar 6;9(5):286-94.

Guy RJ, Dawson JL, Garrett JR, Laws JW, Thomas PK, Sharma AK, Watkins PJ. Diabetic gastroparesis from autonomic neuropathy: surgical considerations and changes in vagus nerve morphology. J Neurol Neurosurg Psychiatry. 1984 Jul;47(7):686-91.

Hall JE. Guyton & Hall: Tratado de Fisiologia Médica. 12ª ed. Rio de Janeiro: Elsevier; 2011.

Hong S, Morrow TJ, Paulson PE, Isom LL, Wiley JW. Early painful diabetic neuropathy is associated with differential changes in tetrodotoxin sensitive and -resistant sodium channels in dorsal root ganglion neurons in the rat. J Biol Chem. 2004 Jul 9;279(28):29341-50.

Horowitz M, Jones KL, Akkermans LMA, Samson M: Gastric function. In: Gastrointestinal Function in Diabetes Mellitus. Edited by Horowitz M, Samsom M. Chichester: John Wiley and Sons, 2004. Cap. 4, p. 117–176.

Horváth VJ, Putz Z, Izbéki F, Körei AE, Gerő L, Lengyel C, Kempler P, Várkonyi T. Diabetes-related dysfunction of the small intestine and the colon: focus on motility. Curr Diab Rep. 2015 Nov;15(11):94.

Huang Y, Zang Y, Zhou L, Gui W, Liu X, Zhong Y. The role of TNF-alpha/NF-kappa B pathway on the up-regulation of voltage-gated sodium channel Nav1.7 in DRG neurons of rats with diabetic neuropathy. Neurochem Int. 2014 Sep;75:112-9.

Kamenov ZA, Traykov LD. Diabetic autonomic neuropathy. Adv Exp Med Biol. 2012;771:176-93.

Nakajima K, Tooyama I, Yasuhara O, Aimi Y, Kimura, H. Immunohistochemical demonstration of choline acetyltransferase of a peripheral type (pChAT) in the enteric nervous system of rats. J Chem Neuroanat. 2000 Feb;18(1-2):31-40.

Oda Y. Choline acetyltransferase: The structure, distribution and phatologic changes in the central nervous system. Pathol Int. 1999 Nov;49(11):921-37.

Regalia J, Cai F, Helke C. Streptozotocin-induced diabetes and the neurochemistry of vagal afferent neurons. Brain Res. 2002 May 31;938(1-2):7-14.

Rodrigues MLC, Motta, MEFA. Mechanisms and factors associated with gastrointestinal symptoms in patients with diabetes mellitus. J Pediatr (Rio J). 2012 Jan-Feb;88(1):17-24.

Sage D, Salin P, Alcaraz G, Castets F, Giraud P, Crest M et al. Na(v)1.7 and Na(v)1.3 are the only tretodotoxin-sensitive sodium channels expressed by the adult guinea pig enteric nervous system. J Comp Neurol. 2007 Oct 1;504(4):363-78.

Sanders KM, Koh SD, Ward SM. Interstitial cells of cajal as pacemakers in the gastrointestinal tract. Annu Rev Physiol. 2006;68:307-43.

Seuring T, Archangelidi O, Suhrcke M. The economic costs of type 2 diabetes: a global systematic review. Pharmacoeconomics. 2015 Aug;33(8):811-31.

Smith B. Neuropathology of the esophagus in diabetes mellitus. J Neurol Neurosurg Psychiatry. 1974 Oct;37(10):1151-4.

Surendran S, Kondopaka SB. Altered expression of neuronal nitric oxide synthase in the duodenum longitudinal muscle-myenteric plexus of obesity induced diabetes mouse: Implications on enteric neurodegeneration. Biochem Biophys Res Commun. 2005 Dec 16;338(2):919-22.

Tan AM, Samad OA, Dib-Hajj SD, Waxman SG. Virus-mediated knockdown of Nav1.3 in dorsal root ganglia of STZ-induced diabetic rats alleviates tactile allodynia. Mol Med. 2015 Jun 18;21:544-52.

Thuneberg L. Interstitial cells of Cajal: intestinal pacemaker cells? Adv Anat Embryol Cell Biol. 1982;71:1-130.

Uesaka T, Young HM, Pachnis V, Enomoto H. Development of the intrinsic and extrinsic innervation of the gut. Dev Biol. 2016 Sep 15;417(2):158-67.

Ward SM, Beckett EA, Wang X, Baker F, Khoyi M, Sanders KM. Interstitial cells of Cajal mediate cholinergic neurotransmission from enteric motor neurons. J Neurosci. 2000 Feb 15;20(4):1393-403.

Ward SM, McLaren GJ, Sanders KM. Interstitial cells of Cajal in the deep muscular plexus mediate enteric motor neurotransmission in the mouse small intestine. J Physiol. 2006 May 15;573(Pt 1):147-59.

Waxman SG, Kocsis JD, Black JA. Type III sodium channel mRNA is expressed in embryonic but not adult spinal sensory neurons, and is reexpressed following axotomy. J Neurophysiol. 1994 Jul;72(1):466-70.

Yarandi SS, Srinivasan S. Diabetic gastrointestinal motility disorders and the role of enteric nervous system: current status and future directions. Neurogastroenterol Motil. 2014 May;26(5):611-24.

Zanoni JN, Miranda-Neto MH, Bazotte RB, Souza RR. Morphological and quantitative analysis of the neurons of the myenteric plexus of the cecum of streptozotocin-induced diabetic rats. Arq Neuropsiquiatr. 1997 Dec;55(4):696-702.

Zhao J, Liao D, Yang J, Gregersen H. Biomechanical remodeling of the diabetic gastrointestinal tract. In: Levy JH. Biomechanics: Principles, Trends and Applications. USA, 2010. Cap. 5, p. 137-162.

APÊNDICE A - Artigo

Effects of diabetes mellitus on myenteric neuronal density and sodium channel expression in the rat ileum

Amanda Damasceno Brasileiro[a], Lidiane Pereira Garcia[a], Samuel de Carvalho da Silva[a], Lenaldo Branco Rocha[a], André Luiz Pedrosa[a], André Shwambach Vieira[a], Valdo José Dias da Silva[a], Aldo Rogelis Aquiles Rodrigues[a]

[a]Institute of Biological and Natural Science, Federal University of Triângulo Mineiro, Uberaba, Minas Gerais, Brazil.

Corresponding author

Aldo Rogelis Aquiles Rodrigues

Universidade Federal do Triângulo Mineiro

Praça Manoel Terra, N° 330, CEP 38025-015, Uberaba, Minas Gerais, Brasil

E-mail address: aldo.rodrigues@uftm.edu.br

ABSTRACT

Diabetes mellitus (DM) may lead to gastrointestinal motility disorders. Rodent models of DM indicate the presence of morpho-functional abnormalities of the enteric nervous system. Here, we evaluated whether experimental DM can cause changes in the excitatory cholinergic fibers, neuronal density, and voltage-gated sodium channel (Nav) expression in the myenteric plexus of the ileum. After streptozotocin-induced hyperglycemia in female rats progressed for eight weeks, triple immunofluorescence labeling experiments revealed that the neuronal density in DM rats was significantly lower than that in control. On average, the density of total neurons reduced by 52.2% ($p = 0.0001$), cholinergic neurons by 50.0% ($p = 0.0068$), and nitrergic neurons by 54.8% ($p = 0.0042$). The number of neurons per ganglionic area was also significantly reduced (to 28.2% of total neurons, $p = 0.0002$; 27.7% of cholinergic neurons, $p = 0.0002$, and 32.1% of nitrergic neurons, $p = 0.0016$). Furthermore, the density of the cholinergic fibers at the surface of the longitudinal muscle was significantly reduced (DM: 24 ± 3%; $p = 0.003$, control: 41 ± 2%); however, western-blot analysis did not indicate a reduction in the expression of choline acetyltransferase (ChAT) in the DM group. The Nav1.6 isoform was detected in different myenteric neurons of the ileum. RT-qPCR data did not suggest an alteration of transcripts for ChAT, neuronal nitric oxide synthase, Nav1.3, Nav1.6, or Nav1.7. Our data support the view that chronic DM leads to a reduction of excitatory cholinergic fibers and neuronal density. However, changes in sodium channel expression pattern, which could cause neuronal dysfunction, were not detected.

Keywords: Diabetes mellitus; Enteric nervous system; Sodium channels; Gastrointestinal disorders; Cholinergic neurons; Nitrergic neurons.

1. INTRODUCTION

Diabetes mellitus (DM) can affect gastrointestinal function, causing nausea, vomiting, diarrhea, constipation, dyspepsia, fecal incontinence, or a combination of these symptoms (Gotfried et al., 2017), which impairs the quality of life of patients (Zhao et al., 2017). One of the structures that might possibly be affected by diabetic neuropathy is the myenteric plexus, which is a part of the enteric nervous system (ENS) located between the circular and longitudinal muscular layers and extends from the esophagus to the rectum (Furness, 2012). Indeed, some studies have linked a reduction in neuronal density in the intestinal myenteric plexus of rats to manifestations of diabetic neuropathy (Pereira et al., 2011; Pereira et al., 2016; Panizzon et al., 2016).

Voltage-dependent sodium channels (Nav) are involved in the initiation and propagation of action potentials in neurons. At least nine subtypes of Nav, named Nav1.1 to Nav1.9, are found to be heterogeneously distributed in mammalian tissues (Catterall et al., 2017). In the ENS of guinea pigs, the transcripts for Nav1.2, 1.3, 1.6, and 1.7 isoforms, known as tetrodotoxin-sensitive sodium channels, were detected (Bartoo et al., 2005). Additionally, the authors detected Nav1.2 immunoreactivity at the somata, Nav1.3 in the dendrites, somata, and the fibers that interconnect the myenteric plexus ganglia, and Nav1.6 at the initial segment of the axon. Nav1.6 was observed only in the neurons of the colon and not in the myenteric plexus of the small intestine. Sage et al. (2007), using different molecular techniques, demonstrated the expression of Nav1.3 and Nav1.7 in neurons of the duodenal myenteric plexus of guinea pigs, although both could not be detected by immunohistochemistry.

In the dorsal root ganglion neurons (DRG), Nav1.3 is expressed at the early stages of neuronal development and is not observed in adult rats. Interestingly, these channels are expressed again after peripheral axotomy (Waxman et al., 1994). Other studies have shown that Nav1.3 expression is up-regulated in DRG neurons in cases of nerve damage (Black et al., 1999) and in neuropathic pain associated with diabetes (Craner et al., 2002; Tan et al., 2015; Yang et al., 2016). There is evidence that diabetic neuropathy may lead to increased (Craner et al., 2002) or decreased (Hong et al., 2004) expression of the Nav1.6 isoform in DRG neurons, whereas Nav1.7 expression seems to be increased (Huang et al., 2014). Although it is possible to link changes in sodium channel expression to diabetic neuropathy in neurons of the DRG, we have not found any study that evaluated

sodium channel expression in enteric neurons during the progression of chronic diabetes. If DM could change the expression of sodium channels in enteric neurons, this could cause abnormal neuronal excitability. The functional outcome of these changes will depend on which neurons are most affected by neuropathy within the different neuronal circuits of the ENS. It is well known that the myenteric plexus is composed of a large diversity of neurons, e.g. sensory neurons, interneurons, and excitatory and inhibitory motor neurons (Furness, 2012). Thus, determining whether a subtype of neuron is affected by this specific mechanism may allow the development of therapeutic strategies targeting sodium channel dysfunction. These findings will contribute to the understanding of the mechanisms of neuropathy in the ENS.

The present study aimed to evaluate whether DM causes alterations in the expression of voltage-gated sodium channels in ENS neurons. To increase the understanding of enteric neuropathy and as a basis for detailed evaluation of possible changes in the expression of sodium channels in our experimental model, we additionally evaluated whether DM affects excitatory cholinergic fibers and neuronal density or induces morphological changes in the distal ileum of rats.

2. RESULTS

To monitor the glycemic levels of control and DM rats, a fasting blood glucose measurement was performed weekly. The analysis of glycemic values in the two experimental groups indicated a significant increase from baseline in the DM group after the first week of streptozotocin administration and during the period of observation (Figure 1A). In the control group, glycemia tended to decrease over the experimental period, being lower in the seventh and eighth weeks than at baseline. In the DM group, rats displayed a significant loss of weight in the second and third week, a slight recovery in the fourth week, followed by further reduction of body weight. In the control group, a progressive gain of weight was observed, being significantly higher in the eighth week compared to baseline (Figure 1B).

Aiming to evaluate whether DM leads to a reduction of the excitatory projections to the smooth muscle, we analyzed the density of thin cholinergic fibers on the surface of the longitudinal smooth muscle. In the DM group, there was a significant reduction in the percentage density of these fibers relative to control (control: 41 ± 2%, DM: 24 ± 3%; p =

0.003), as shown in figure 2A, B, and C. To further evaluate the cholinergic innervation, we performed western blot experiments for choline acetyltransferase (ChAT). Results shown in figure 2D indicate no differences in the relative expression of ChAT between rats in the control and DM groups. The inset shows a representative result of ChAT labeling of cerebral tissue, used as a positive control for ChAT expression, and of the distal ileum from both experimental groups. The absence of labeling when the primary antibody was omitted from the reaction is also shown.

Triple immunofluorescence labeling experiments were performed to evaluate the effect of DM on the neuronal density of the myenteric plexus (Figure 3). A representative labeling result is shown for the anti-pan neuronal marker HuC/HuD at the neuronal somata and nuclei (Figure 3A and 3E), anti-ChAT at somata and processes of distinct neurons (3B and 3F), anti-nNOS (neuronal nitric oxide synthase; 3C and 3G), and the merged figure for these images (3D and 3H) for control and DM groups, respectively. We observed a significant reduction of the mean neuronal density for total (control: 20671 ± 1562, DM: 9887 ± 879; p = 0.0001), cholinergic (control: 15268 ± 1991, DM: 7635 ± 849; p = 0.068), and nitrergic neurons (control: 4843 ± 596, DM: 2190 ± 385; p = 0.0042) in the DM group compared to the control group (Figure 3I) when the analysis was performed in the area of the longitudinal muscle/myenteric plexus (LMMP). Although not illustrated, the mean circumference length of the ileal wall in the DM group was significantly larger than that in the control group (control: 1.60 ± 0.04 cm, n = 11; DM: 2.21 ± 0.08, n = 9, p = 4.6×10^{-6}), indicating a circular distension that could reduce the neuronal density per se. Therefore, we also analyzed the neuronal density per ganglionic area. Reductions of neuronal density of total (control: 238115 ± 12234, DM: 170846 ± 11284; p = 0.0002), cholinergic (control: 178007 ± 9084, DM: 128622 ± 7729; p = 0.0002), and nitrergic neurons (control: 54441 ± 4012, DM: 36979 ± 3461; p = 0.0016) were also observed in the area of the ganglia in the DM group compared to the control group (Figure 3J). The proportions of cholinergic and nitrergic neurons in relation to the total number of neurons remained the same in both experimental groups when analysis was performed in the ganglionic area for ChAT (control: 74.7 ± 1.1%, DM: 74.8 ± 0.9%; p = 0.9) and for nNOS (control: 23.2 ± 1.4%, DM: 22 ± 1.3%; p = 0.5), as indicated in Figure 3K or the wall area of the LMMP (not shown). The average ganglion size in control (9891 ± 1986 μm^2) and DM rats (11309 ± 1100 μm^2) was not significantly different (p = 0.5) as shown in Figure 3L.

To establish a positive control for our immunolabeling experiments for Nav1.6 antibodies before performing experiments in the myenteric plexus, we used slices of the cerebellum (Figure 4), as the expression of this subtype of sodium channels has been well characterized in the Purkinje cells (Jenkins et al., 2001). The anti-Nav1.6 antibody (Alomone) produced intense labeling along the axon initial segment of Purkinje cells (arrows in Figure 4B), which was not labeled by the anti-MAP-2 antibody, a marker of dendrites and cell bodies (Figure 4A and C). Pre-incubation of the antibody with the antigenic peptide abolished the labeling and resulted in the negative control image (Figure 4D).

Using the LMMP preparation of the ileum, we found anti-Nav1.6 labeling in both, non-cholinergic and cholinergic neurons (Figure 5A, B, and C for control and Figure 5D, E, and F for DM group). The anti-Nav1.6 labeling was observed on the cell somata as well as its processes. We sought to compare the size of neurons exhibiting positive labeling for Nav1.6 in control and DM rats. To this end, we performed an analysis of the somatic silhouette area of Nav1.6 positive neurons in both groups (Figure 5G). The frequency plot histogram confirms that the size of Nav1.6 positive neurons was heterogeneous in the enteric neurons from control and DM rats. In the DM group, the size variation of Nav1.6-positive neurons was less pronounced and shifted towards larger sizes, but the differences were not significant (control: 297.4 ± 10 μm^2, DM: 372.5 ± 8.4 μm^2, $p = 0.3$). Additionally, we detected the expression of Nav1.6 using a polyclonal anti-Nav1.6 antibody (Alomone) and a monoclonal antibody (Neuromab) in cryosections (data not shown). We did not detect immunoreactivity for Nav1.3 and Nav1.7.

We have also analyzed the expression of ChAT, nNOS, and sodium channels in these neurons using RT-qPCR reactions (Figure 6). To better illustrate the results, we plotted the mean and standard deviation of the ΔCt value for each gene in the control and DM groups (Figure 6A). Comparisons of fold change values indicated that the only gene with reduced expression in the DM group was Nav1.6, although none of the studied genes showed significantly changes in expression (Figure 6B).

3. DISCUSSION

In this study, we used a single intraperitoneal administration of streptozotocin to induce lesions of pancreatic beta cells in rats. Seven days after this administration, the rats

developed significant hyperglycemia that slowly increased during the experimental period, suggesting a progression of beta-cell lesions. During this period of eight weeks, the DM rats also underwent significant weight loss, resembling uncontrolled type 1 diabetes in humans. Previous data suggest that the presence of a constant hyperglycemic state is associated with a reduction of total, excitatory, and inhibitory neurons in the male rat colon (Du et al., 2009) and the male mouse ileum (Domènech et al., 2011). Peripheral neuropathy seems to affect male and female rats similarly (Coppey et al., 2018); however, the number of studies that explored gender differences or evaluated enteric neuropathy in female rodents is limited. Therefore, to accumulate more data about the effects of DM in females, we opted to use female rats in this study. Enteric neuropathy induces modifications in the gastrointestinal tract, such as relaxation of the lower esophageal sphincter, gastroesophageal reflux (Yarandi & Srinivasan, 2014), gastroparesis (Uranga-Ocio et al., 2015), and, finally, delayed gastric emptying that is attributed to the loss of nitrergic innervation in the gastric fundus (Rodrigues & Motta, 2012). However, the exact effects and the mechanisms by which DM affects the small and the large intestines remain unclear.

Our immunostaining data revealed a significant reduction in the density of thin cholinergic fibers in the longitudinal smooth muscle in the DM group in relation to control group. Most of these fibers constitute the tertiary plexus that are involved in the innervation of smooth muscle cells at the surface of the longitudinal muscle layer (Llewellyn-Smith et al., 1993). A reduction in the density of these fibers in the DM group could lead to a reduction in excitatory efference. On the other hand, no significant change in ChAT enzyme expression was observed in western blotting experiments. It is important to consider that the homogenate included all the submucosal and myenteric plexus structures (ganglia, primary, secondary, and tertiary fibers), making a direct comparison between enzyme expression and tertiary fiber density difficult.

A significant reduction in the density of the three evaluated neuronal populations, including the total, cholinergic, and nitrergic neurons in the ileal myenteric plexus was observed in our triple immunofluorescence results. The circumferential length of the ileal segments was significantly higher (72.3%) in animals with DM than in control animals, which was similar to the results observed by Mayhew et al. (1989), suggesting an intestinal smooth muscle distention. Differences in the circumferential length may also reflect

different contractile responses during tissue collection or assembly. However, we used inhibitors of contraction (atropine and nifedipine) during tissue collection to minimize the consequences of this effect. With respect to the total length of the small intestine, some authors observed an increase, for example, by 17.8% after three weeks of diabetes (Nakabou et al., 1974) or by 16.5% after nine weeks of diabetes (Honoré et al., 2011). Thus, a neuronal density estimation would require a two-dimensional correction factor for a reliable comparison between the DM and control groups. Although the transverse factor was readily obtained, the longitudinal direction factor was challenging to obtain, since an increase in the total length of the small intestine does not necessarily indicate an increase of the ileal length. Thus, the reduced density of the neuronal or fine cholinergic fibers in the DM group, which is based on the LMMP area, should be interpreted with caution.

Due to the difficulties in circumventing some experimental variables that may have interfered with the ileal wall area, we opted to analyze the number of neurons per ganglionic area, as suggested by Karaosmanoglu et al. (1996). According to these authors, the area of the ganglia does not change when the intestinal wall is stretched. Using this alternative method of analysis in our study, a significant reduction in neuronal density was observed in animals in the DM group relative to the control group, while the average ganglion size was not changed. Panizzon et al. (2016) also described a significant reduction in total neuronal density (HuC/HuD positive) in the ileum of diabetic rats using this method. In addition, it was observed that there was no difference in the proportions of cholinergic or nitrergic neurons in relation to the total number of neurons between the groups, suggesting that there is no preferential loss of a specific neuronal subtype analyzed in diabetes in the experimental time evaluated.

The anti-Nav1.6 antibody most used in our experiments (Alomone) has been shown to detect the Nav1.6 channel in different neurons in the cortex and the hippocampus (Liu et al., 2017). The expression of Nav1.6 in Purkinje cells of the cerebellum is well-established in the literature, for instance using the antibody from Neuromab (Osorio et al., 2010). Using these antibodies and a protocol for fixation that preserve antigenicity (McLean & Nakane, 1974), we have detected the Nav1.6 isoform in myenteric neurons of rats (control and DM) in cell somata as well as in the processes derived from soma, indicating that Nav1.6 channels are evenly distributed along the cell surface. This labeling pattern was different from that observed in the Purkinje cells where the channels are

concentrated at axon initial segments. The labeling in myenteric neurons was detected in neurons of different sizes and morphology, and in both, cholinergic and non-cholinergic neurons. In contrast, Sage et al. (2007) could not detect immunoreactivity for Nav1.6 in the myenteric neurons of guinea pigs. It is important to point out that they have used the same antibody (Alomone) and dilution (1:100) as in our current study. When they increased the antibody concentration to 1:50, labeling was found in glial cells. Considering that we detected anti-Nav1.6 labeling in neurons of the rat ileum using two well-known antibodies, we hypothesize that the different results reflect species differences. Additional studies are necessary to clarify this issue and to characterize the Nav1.6 expressing neurons in the ENS. The data showing that the size of Nav1.6 neurons is shifted towards larger neurons in DM group may suggest that the small Nav1.6-positive neurons are more susceptible to DM or that sodium channel expression is changed in smaller Nav1.6-positive neurons during the development of this disease. In our experiments, similar to what was observed by Sage et al. (2007), no immunoreactivity for Nav1.7 was detected. Furthermore, we did not observe anti-Nav1.3 labeling at the myenteric neurons of the ileum in the DM or control groups. This is in contrast to Bartoo et al. (2005) who, using the same antibody, detected Nav1.3 in the guinea pig ileum.

In the RT-qPCR experiments, the housekeeping gene hypoxanthine guanine phosphoribosyltransferase (HPRT1) was chosen since it is not affected by the hyperglycemic state and can be used for studies in populations with type 1 DM (Kar et al., 2016) or during hypoxia (Julian et al. 2014). Despite the significant reduction in DM neuronal density in relation to the control group, the estimated quantities of ChAT and nNOS did not significantly differ between the DM and the control group. Although the terminology for the neuronal NOS isoform suggests selective expression in neurons (Förstermann et al., 1994), this enzyme is also detected in other cells, including cardiac myocytes (Xu et al., 1999) and epithelial cells of different organs (Schmidt et al., 1992; Förstermann e Sessa, 2012). In this context, our data indicate a greater amount of transcript for nNOS than for ChAT, suggesting that other cells in the ileum wall may contribute to an increase in the amount of the transcript for this enzyme. However, the labeling pattern in immunofluorescence reactions is restricted to neurons, similar to the findings of other studies (Van Geldre et al., 2004). Thus, RT-qPCR data do not allow the conclusion that significant changes occur in the expression of enzymes involved in the

synthesis of neurotransmitters in the ENS of the ileum of DM rats, despite a significant reduction in neuronal density.

With respect to transcripts encoding sodium channels, Nav1.6 demonstrated a tendency to be reduced, whereas Nav1.3 and Nav1.7 showed a tendency to be increased in diabetes. The Nav1.3 channel exhibits a slow inactivation from the closed state and a fast recovery from the inactivated state, contributing to low-threshold and high-frequency repetitive action potential firing in neurons (Cummins et al., 2001). The slow closed-state inactivation of Nav1.7 is thought to play an important role in the amplification of subthreshold depolarization and the initiation of action potential firing in neurons (Blair & Bean, 2002; Cummins et al., 2007). Therefore, an increase in the expression of these channels in DM could lead to an increased excitability of enteric neurons.

To our knowledge, our data demonstrate for the first time the expression of Nav1.6 in enteric neurons of the rat ileum using both RT-qPCR and immunofluorescence. This isoform is abundantly expressed in the neurons of the central nervous system where they are expressed at high levels in the initial segments of the axons and are responsible for initiating the action potential in different neurons (Boiko et al., 2003; Raman et al., 1997). The reduction in the amount of Nav1.6 transcripts in ileal homogenates from rats in the DM group may indicate a reduction in the expression of this gene in individual neurons or degeneration of neurons expressing this channel. Electrophysiological experiments combined with single-cell RT-qPCR, in an identified neuron subtype that expresses Nav1.6, could clarify this question. It would be interesting to extend this analysis to other Nav-subtypes that are also detected in enteric neurons in future studies.

4. MATERIAL AND METHODS

4.1 ANIMALS

All procedures were approved by the Ethics Committee on the Use of Animals of the Federal University of Triângulo Mineiro under the protocols 233 and 383. We used thirty 120-day old female Wistar rats (*Rattus norvegicus*) with an average weight of 230 g. The animals were randomly divided into control and diabetes mellitus (DM) groups and kept in groups of three animals per plastic box, in a room with a light-dark cycle of 12 h/12 h (light on at 7 am), temperature of 22 ± 1ºC, and humidity of 40–70%. Normocaloric food (Nuvilab CR1) and water were available *ad libitum* during all experiments, except for

daytime restriction of eight hours on the days on which the glucose levels were measured, or for nine hours on the day of diabetes induction.

4.2 INDUCTION TO DIABETES TYPE 1

Animals of the control (n = 15) and DM (n = 15) groups were weighed and had their glycemia measured in a blood sample from the tail using a glucose meter (Accu Chek® Active, Roche Diagnostics). Subsequently, streptozotocin (STZ, S0130, Sigma) diluted at 4% (w/v) in 0.1 M citrate buffer (pH 4.5) was administered intraperitoneally at a dose of 60 mg/kg of body weight in animals of the DM group. Control animals received only a citrate buffer. After administration, the animals were kept fasting for one hour to avoid the competition of STZ with glucose at the GLUT2 transporter in the pancreatic beta-cells (Szkudelski, 2001). After one week, rats with glycemia equal to or greater than 220 mg/dL were considered as diabetic rats. The fasting glycemia and weight were measured every seven days during the eight weeks of the experiment.

4.3 TISSUE COLLECTION

After the eight-week cycle, the animals were weighed and intraperitoneally anesthetized with Thiopental (Thiopentax, Cristália) at a dose of 40 mg/kg of body weight. After anesthesia was confirmed, a median laparotomy was performed to collect 8 cm of the distal part of ileum, excluding the final 2 cm to avoid the ileocecal junction. Euthanasia of the animals was induced by exsanguination, by cutting either the large vessels of the mesenteric bed or, when necessary, the large cardiac vessels. The collected ileal segment was washed in a phosphate buffered saline (PBS) solution containing (in mM): 142 NaCl, 2.38 KCl, 1.47 KH_2PO_4, 8.06 $NAHPO_4$, pH 7.4, 3 μM of nifedipine, and 1 μM of atropine (51045, Merck). Nifedipine and atropine were used to reduce the constricting response of tissue samples during collection. From the collected segment, the last 2 cm were isolated, frozen in liquid nitrogen, and stored at -80ºC for the RT-qPCR experiments. For immunofluorescence, the remaining segment (approx. 6 cm) was opened at the mesenteric border. To avoid tissue curling, it was attached flat to a wooden board with the aid of pins and then fixed overnight with a fixative solution (2% PLP) containing (in mM): 37 Na_2HPO_4, 75 lysine, 10 sodium metaperiodate (S1878, Sigma), and 2% paraformaldehyde (P6148, Sigma), according to the guidelines by McLean & Nakane

(1974). After fixation, the tissues were washed three times for ten minutes each with dimethyl sulfoxide (D1435, Sigma) and then three times for ten minutes each with PBS solution and stored at 4°C in a solution of PBS and 0.1% sodium azide. For the western-blotting experiments, an 8-cm section of the distal ileum was collected from ten rats (n = 5 for each group) as described above. After washing in PBS, the segment was opened at the mesenteric border and scraped to remove the mucosa, frozen in liquid nitrogen, and stored at -80ºC.

For experiments involving evaluation of the immunolabeling pattern produced by anti-Nav1.6 antibodies, a group of rats (n = 5) was transcardially perfused with PBS followed by the PLP-fixative described above. After that, the brain stem and the cerebellum were removed and post-fixed for four hours in the same fixative and then transferred to a PBS solution containing 30% sucrose at 4ºC. When the block of tissue sunk, it was removed from this solution and stored at -80ºC.

4.4 IMMUNOFLUORESCENCE

For the triple labeling immunofluorescence experiments, segments of 1 cm^2 of the distal ileum were dissected to obtain the whole mount preparation after the removal of the mucosa, submucosa, and circular muscle layer, resulting in isolation of the longitudinal muscle/myenteric plexus (LMMP). The LMMP samples were placed in a blocking/permeabilization buffer containing 1.5% (v/v) Triton X-100 (777, Vetec) and 5% normal donkey serum (NDS, D9663, Sigma) for four hours before placing them in blocking buffer containing 0.5% (v/v) Triton X-100 and 5% NDS plus primary antibodies (1:250) for 36 hours. After washing in PBS, the samples were placed in a blocking buffer along with the secondary antibodies (1:400) for four hours. In case of secondary antibodies obtained from goats instead of donkeys, goat serum (G9023, Sigma) was used for blocking unspecific binding of antibodies. Afterwards, the samples were washed in PBS and mounted on slides with mounting medium (Vectashield, Vector Laboratories). The primary antibodies used were mouse anti-HuC/HuD (A21271, Life Technologies), goat anti-ChAT (AB144P, Millipore), rabbit anti-nNOS (617000, Life Technologies), mouse anti-MAP-2 (MAB378, Millipore), rabbit anti-Nav1.3 (ASC-004, Alomone), rabbit anti-Nav 1.6 (ASC-009, Alomone), mouse anti-Nav 1.6 (75026, Neuromab), and rabbit anti-Nav1.7 (ASC-004, Alomone). The secondary fluorescent antibodies used were: donkey anti-mouse Alexa 568

(A10037, ThermoFisher), donkey anti-goat Alexa 488 (A11055, ThermoFisher), donkey anti-rabbit Alexa 405 (Ab175651, Abcam), goat anti-rabbit Alexa 568, and goat anti-mouse Alexa 488. Images were acquired using a confocal laser scanning microscope (LSM Meta 710, Zeiss) using the 488-nm argon laser line for Alexa 488, the 543-nm helium-neon laser for Alexa 568, and the 405-nm diode laser for Alexa 405. The images (1024 × 1024 pixels) were acquired with a 20x objective (EC Plan-Neofluar, NA: 0.5) for counting the subtypes of neurons or a 40x-oil objective (EC Plan- Neofluor, NA: 1.3) for imaging of the thin cholinergic fibers and single neurons. Analysis of neuronal density was performed by counting the number of neurons per area in images of 0.5 mm^2 of the LMMP or measuring the area of each ganglion and counting the total number of neurons within a ganglion. For each sample (n = 3 per rat of each group), an average number of six fields or eight ganglia were used. For the analysis per ganglionic area, long axis limits for each ganglion were defined as the area where the strand became smaller than the width of two marked neurons in merged images of HuC/HuD and ChAT labeling, as described in Stenkamp-Strahm et al. (2013). For the immunofluorescence analysis of sodium channel antibody-labeling properties of the cerebellum, the experiments were conducted as described above for the LMMP preparations, except that immunofluorescence reactions were developed on slides after cutting slices of 30 µm in a cryostat chamber at -20ºC (CM1850 UV, Leica). The size of Nav1.6-positive neurons was determined by measuring the somatic silhouette area in confocal images and the average size was estimated using 100 neurons in each experimental group.

4.5 SDS-PAGE AND IMMUNOBLOTTING

Fifty milligrams of distal ileum from each animal were homogenized in a weight/volume ratio (g/ml) of 1:10 in 20 mM Tris-HCl buffer, pH 7.4, containing 19 mM EDTA (324503, Merck) and a mixture of proteases inhibitors (P8340, Sigma) diluted at 1:10. The homogenization was done at 1800 rpm (099CK54, Glas-Col) at 4°C for two cycles of ten slow incursions with a one-minute interval between the two. The protein dosage was determined by the Bradford method. The standard curve was made from bovine serum albumin (23236, Thermo Scientific). Absorbance reading at 595 nm was performed in triplicates (BioPhotometer, Eppendorf).

SDS-PAGE was carried out on 10% gradient mini slab gels using a discontinuous system (Laemmli and Favre, 1973). A molecular weight marker (SDS6H2, Sigma) was used as reference (in kDa): porcine myosin II heavy chain (200), *E. coli* ß-galactosidase (116), rabbit muscle phosphorylase b (97.4), bovine serum albumin (66.7), egg albumin (45), and bovine erythrocyte carbonic anhydrase (29).

Western blotting to nitrocellulose membranes (Hybond-C extra, Amersham) was performed according to Towbin et al. (1979). The membrane was treated for two hours for non-specific binding of antibodies with a phosphate buffered solution (mM): 20 Na_2HPO_4, 250 NaCl, 0.1% Triton X-100, pH 7.5, to which 3% BSA solution (A7638, Sigma) was added. The membrane was then treated with primary anti-ChAT antibody (1:1000) overnight. The following day, the membranes were washed three times for five minutes each with the same PBS as described above. The membranes were then incubated for two hours with the secondary donkey anti-goat IgG alkaline phosphatase conjugate (1:500) (Promega, V115A). After washing four times for five minutes each, the membranes were incubated with the color development solution consisting of 100 mM Tris-HCl, 150 mM NaCl, 1 mM $MgCl_2$, and 2 mM of Levamisole, pH 9.5, plus 0.16 mg/ml BCIP (5-bromo-4chloro-3indolyl-phosphate) and 0.33 mg/ml NBT (nitro blue tetrazolium) according to the manufacturer´s instructions (S3771, Promega). The development reaction time was 15 minutes and the reaction was stopped with distilled water. Labeled immunoblots were photographed using the VersaDoc MP500 and its software Quantity One (Bio-Rad Laboratories).

4.6 QUANTITATIVE REVERSE TRANSCRIPTION PCR (RT- qPCR)

Segments of the distal ileum were removed from the –80ºC freezer and transferred to a cryostat chamber kept at –20ºC. After mounting the sample on a specimen holder with Tissue-Tek Compound (4583, Sakura), slices of 8 μm were cut and then diluted in Trizol (15596-026, ThermoFisher,) at a proportion of 50 mg/1 ml. Total RNA was extracted and isolated by the phenol-chloroform method, and its concentration was estimated by measuring the absorbance at 260 nm using a spectrophotometer (NanoDrop, ThermoFisher). RNA samples exhibiting 260/280 absorbance ratio above 1.8 were used. Reverse transcription reactions were performed on 2 μg of total RNA using the High Capacity cDNA Reverse Transcription kit (4368814, ThermoFisher) and the thermal cycler

(MyCycler™ Thermal Cycler, BioRad). The cDNA amplification reactions were performed using the Power Up™ SYBR® Green Master Mix kit (A25741, ThermoFisher) using 5 μl of the kit, 2.5 μl of forward and reverse primers solutions at 3 μM and 2.5 μl of cDNA (70 ng), resulting in 10 μl per well. DEPC-treated water replaced cDNA in negative controls. The amplification reactions were performed in triplicates for each gene studied utilizing a real-time PCR system (StepOnePlus, ThermoFisher). HPRT1 was used as the housekeeping gene. The primer sequences used are shown in Table 1. To confirm that only one product was amplified, a melting curve analysis was performed at the end of each PCR step. The relative quantification of the transcripts was analyzed using the $2^{-\Delta\Delta CT}$ method (fold change) (Livak & Schmittgen, 2001).

Table 1 - Sequences of primers used in RT-qPCR experiments.

Primer	Direction	Sequence	Size (bp)
ChAT	Forward Reverse	TGGCTTACTACAGGCTTTACC AGTGGCTGATCTGATGTTGTC	22 21
nNOS	Forward Reverse	GGCGAACAACTCCCTCATTA TTGGAAAGACCTTGGGTCAG	20 20
Nav1.3	Forward Reverse	ACAACCTCTCCTCCTTCCTAT CTCTCTGACCTCTTTCCCTTTG	21 22
Nav1.6	Forward Reverse	CCCAACCCTATTCCGAGTTATC CAGCGACATCATTAAGGCAAAG	22 22
Nav1.7	Forward Reverse	GTCGTGTCGCTTGTTGATGG CTGATTAGTCGTGCCGCTGT	20 20
HPRT1	Forward Reverse	TCCTCCTCAGACCGCTTTTC ATCACTAATCACGACGCTGGG	20 21

bp: base-pairs

4.7 ANALYSIS AND STATISTICS

ImageJ 1.49t (Schneider et al., 2012) was used for image processing and analyses of immunofluorescence and western-blotting data. Quantification of the optical density for each band in the same membrane was made using the Gels analysis tool. Data were plotted as mean and standard error of the mean unless indicated otherwise. All data were subjected to the normality test of Shapiro-Wilk and homogeneity of variance test of Levene. Student´s t-test was applied to parametric data and Mann–Whitney test to nonparametric data. The significance level was set as 0.05 for all comparisons. The

software Origin 2017 (OriginLab) was used for statistical analyses and graph plotting. Adobe Illustrator CS (Adobe System, USA) was used for figures illustrations.

ACKNOWLEDGMENTS

We wish to thank Glauco da Rocha Findholdt, Angélica Cristina Alves da Cruz, and Lucas Felipe de Oliveira for the technical support.

FUNDING

This work was supported by the Research Support Foundation of Minas Gerais (FAPEMIG). The authors declare that they have no conflict of interest.

REFERENCES

Bartoo AC, Sprunger LK, Schneider DA. Expression and distribution of TTX sensitive sodium channel alpha subunits in the enteric nervous system. J Comp Neurol. 2005 May 30;486(2):117-31. DOI: 10.1002/cne.20541.

Black JA, Cummins TR, Plumpton C, Chen YH, Hormuzdiar W, Clare JJ et al. Upregulation of a silent sodium channel after peripheral, but not central, nerve injury in DRG neurons. J Neurophysiol. 1999 Nov;82(5):2776-85. DOI: 10.1152/jn.1999.82.5.2776.

Blair NT, Bean BP. Roles of tetrodotoxin (TTX)-sensitive Na^+ current, TTX-resistant Na^+ current, and Ca^{2+} current in the action potentials of nociceptive sensory neurons. J Neurosci. 2002 Dec;22(23):10277-90.

Boiko T, Van Wart A, Caldwell JH, Levinson SR, Trimmer JS, Matthews G. Functional specialization of the axon initial segment by isoform-specific sodium channel targeting. J Neurosci. 2003 Mar 15;23(6):2306-13. DOI: 10.1523/JNEUROSCI.23-06-020306.2003.

Catterall WA, Goldin AL, Waxman SG. Guide to pharmacology [www.guidetopharmacology.org]. Voltage-gated sodium channels: introduction. Last modified on 03/22/2017. Accessed on 08/23/2018. Available at: www.guidetopharmacology.org/GRAC/FamilyIntroductionForward?familyid=82.

Coppey LJ, Shevalye H, Obrosov A, Davidson EP, Yorek MA. Determination of peripheral neuropathy in high-fat diet fed low-dose streptozotocin-treated female C57Bl/6J mice and Sprague-Dawley rats. J Diabetes Investig. 2018 Feb 7. DOI: 10.1111/jdi.12814.

Craner MJ, Klein JP, Renganathan M, Black JA, Waxman SG. Changes of sodium channel expression in experimental diabetic neuropathy. Ann Neurol. 2002 Dec;52(6):786-92. DOI: 10.1002/ana.10364.

Cummins TR, Aglieco F, Renganathan M, Herzog RI, Dib-Hajj SD, Waxman SG. Nav1.3 sodium channels: rapid repriming and slow closed-state inactivation display quantitative differences after expression in a mammalian cell line and in spinal sensory neurons. J Neurosci. 2001 Aug 15;21(16):5952-61. DOI: 10.1523/JNEUROSCI.21-16-05952.2001.

Cummins TR, Sheets PL, Waxman SG. The roles of sodium channels in nociception: Implications for mechanisms of pain. Pain. 2007 Oct;131(3):243-57. DOI: 10.1016/j.pain.2007.07.026.

Domènech A, Pasquinelli G, De Giorgio R, Gori A, Bosch F, Pumarola M et al. Morphofunctional changes underlying intestinal dysmotility in diabetic RIP-*I*hIFNb transgenic mice. Int J Exp Pathol. 2011 Dec;92(6):400-12. DOI: 10.1111/j.1365-2613.2011.00789.x.

Du F, Wang L, Qian W, Liu S. Loss of enteric neurons accompanied by decreased expression of GDNF and PI3K/Akt pathway in diabetic rats. Neurogastroenterol Motil. 2009 Nov;21(11):1229-e114. DOI: 10.1111/j.1365-2982.2009.01379.x.

Förstermann U, Closs EI, Pollock JS, Nakane M, Schwarz P, Gath I et al. Nitric oxide synthase isozymes. Characterization, purification, molecular cloning, and functions. Hypertension. 1994 Jun;23(6 Pt 2):1121-31. DOI: 10.1161/01.HYP.23.6.1121.

Förstermann U, Sessa WC. Nitric oxide synthases: regulation and function. Eur Heart J. 2012 Apr;33(7):829-37, 837a-837d. DOI: 10.1093/eurheartj/ehr304.

Furness JB. The enteric nervous system and neurogastroenterology. Nat Rev Gastroenterol Hepatol. 2012 Mar 6;9(5):286-94. DOI: 10.1038/nrgastro.2012.32.

Gotfried J, Priest S, Schey R. Diabetes and the Small Intestine. Curr Treat Options Gastroenterol. 2017 Dec;15(4):490-507. DOI: 10.1007/s11938-017-0155-x.

Hong S, Morrow TJ, Paulson PE, Isom LL, Wiley JW. Early painful diabetic neuropathy is associated with differential changes in tetrodotoxin sensitive and -resistant sodium channels in dorsal root ganglion neurons in the rat. J Biol Chem. 2004 Jul 9;279(28):29341-50. DOI: 10.1074/jbc.M404167200.

Honoré SM, Zelarayan LC, Genta SB, Sánchez SS. Neuronal loss and abnormal BMP/Smad signaling in the myenteric plexus of diabetic rats. Auton Neurosci. 2011 Oct 28;164(1-2):51-61. DOI: 10.1016/j.autneu.2011.06.003.

Huang Y, Zang Y, Zhou L, Gui W, Liu X, Zhong Y. The role of TNF-alpha/NF-kappa B pathway on the up-regulation of voltage-gated sodium channel Nav1.7 in DRG neurons of rats with diabetic neuropathy. Neurochem Int. 2014 Sep;75:112-9. DOI: 10.1016/j.neuint.2014.05.012.

Jenkins SM, Bennett V. Ankyrin-G coordinates assembly of the spectrin-based membrane skeleton, voltage-gated sodium channels, and L1 CAMs at Purkinje neuron initial segments. J Cell Biol. 2001 Nov 26;155(5):739-46. DOI: 10.1083/jcb.200109026.

Julian GS, de Oliveira RW, Perry JC, Tufik S, Chagas JR. Validation of housekeeping genes in the brains of rats submitted to chronic intermittent hypoxia, a sleep apnea model. PLoS One. 2014 Oct 7;9(10):e109902. DOI: 10.1371/journal.pone.0109902

Kar P, Chawla H, Saha S, Tandon N, Goswami R. Identification of reference housekeeping-genes for mRNA expression studies in patients with type 1 diabetes. Mol Cell Biochem. 2016 Jun;417(1-2):49-56. DOI: 10.1007/s11010-016-2712-3.

Karaosmanoglu T, Aygun B, Wade PR, Gershon MD. Regional differences in the number of neurons in the myenteric plexus of the guinea pig small intestine and colon: an evaluation of markers used to count neurons. Anat Rec. 1996 Apr;244(4):470-80. DOI: 10.1002/(SICI)1097-0185(199604)244:4<470.

Laemmli UK, Favre M. Maturation of the head of bacteriophage T4. I. DNA packaging events. J Mol Biol. 1973 Nov 15;80(4):575-99. DOI: 10.1016/0022-2836(73)90198-8.

Liu Y, Lai S, Ma W, Ke W, Zhang C, Liu S et al. CDYL suppresses epileptogenesis in mice through repression of axonal Nav1.6 sodium channel expression. Nat Commun. 2017 Aug 25;8(1):355. DOI: 10.1038/s41467-017-00368-z.

Livak KJ, Schmittgen TD. Analysis of relative gene expression data using real-time quantitative PCR and the $2^{-\Delta\Delta CT}$ method. Methods. 2001 Dec;25(4):402-8. DOI: 10.1006/meth.2001.1262.

Llewellyn-Smith IJ, Costa M, Furness JB, Bornstein JC. Structure of the tertiary component of the myenteric plexus in the guinea-pig small intestine. Cell Tissue Res. 1993 Jun;272(3):509-16. DOI: 10.1016/0022-2836(73)90198-8.

Mayhew TM, Carson FL, Sharma AK. Small intestinal morphology in experimental diabetic rats: a stereological study on the effects of an aldose reductase inhibitor (ponalrestat) given with or without conventional insulin therapy. Diabetologia. 1989 Sep;32(9):649-54. DOI: 10.1007/BF00274251.

McLean IW, Nakane PK. Periodate-lysine-paraformaldehyde fixative. A new fixation for immunoelectron microscopy. J Histochem Cytochem. 1974 Dec;22(12):1077-83. DOI: 10.1177/22.12.1077.

Nakabou Y, Okita C, Takano Y, Hagihira H. Hyperplastic and hypertrophic changes of the small intestine in alloxan diabetic rats. J Nutr Sci Vitaminol (Tokyo). 1974;20(3):227-34. DOI: 10.3177/jnsv.20.227.

Osorio N, Cathala L, Meisler MH, Crest M, Magistretti J, Delmas P. Persistent Nav1.6 current at axon initial segments tunes spike timing of cerebellar granule cells. J Physiol. 2010 Feb 15;588(Pt 4):651-70. DOI: 10.1113/jphysiol.2010.183798.

Panizzon CPNB, Zanoni JN, Hermes-Uliana C, Trevizand AR, Sehabere CV, Pereira RVF et al. Desired and side effects of the supplementation with l-glutamine and l-glutathione in enteric glia of diabetic rats. Acta Histochem. 2016 Jul;118(6):625-631. DOI: 10.1016/j.acthis.2016.07.008.

Pereira RV, Tronchini EA, Tashima CM, Alves EP, Lima MM, Zanoni JN. L-glutamine supplementation prevents myenteric neuron loss and has gliatrophic effects in the ileum of diabetic rats. Dig Dis Sci. 2011 Dec;56(12):3507-16. DOI: 10.1007/s10620-011-1806-8.

Pereira RV, Linden DR, Miranda-Neto MH, Zanoni JN. Differential effects in CGRPergic, nitrergic, and VIPergic myenteric innervation in diabetic rats supplemented with 2% L-glutamine. An Acad Bras Cienc. 2016;88 Suppl 1:609-22. DOI: 10.1590/0001-3765201620150228.

Raman IM, Sprunger LK, Meisler MH, Bean BP. Altered subthreshold sodium currents and disrupted firing patterns in Purkinje neurons of Scn8a mutant mice. Neuron. 1997 Oct;19(4):881-91. DOI: 10.1016/S0896-6273(00)80969-1.

Rodrigues MLC, Motta, MEFA. Mechanisms and factors associated with gastrointestinal symptoms in patients with diabetes mellitus. J Pediatr (Rio J). 2012 Jan-Feb;88(1):17-24. DOI:10.2223/JPED.2153.

Sage D, Salin P, Alcaraz G, Castets F, Giraud P, Crest M et al. Na(v)1.7 and Na(v)1.3 are the only tretodotoxin-sensitive sodium channels expressed by the adult guinea pig enteric nervous system. J Comp Neurol. 2007 Oct 1;504(4):363-78. DOI: 10.1002/cne.21450.

Schneider CA, Rasband WS, Eliceiri KW. NIH Image to ImageJ: 25 years of image analysis. Nat Methods. 2012 Jul;9(7):671-5. DOI: 10.1038/nmeth.2089.

Stenkamp-Strahm CM, Kappmeyer AJ, Schmalz JT, Gericke M, Balemba O. High-fat diet ingestion correlates with neuropathy in the duodenum myenteric plexus of obese mice with symptoms of type 2 diabetes. Cell Tissue Res. 2013 Nov;354(2):381-94. DOI: 10.1007/s00441-013-1681-z.

Szkudelski T. The mechanism of alloxan and streptozotocin action in B cells of the rat pancreas. Physiol Res. 2001;50(6):537-46.

Tan AM, Samad OA, Dib-Hajj SD, Waxman SG. Virus-mediated knockdown of Nav1.3 in dorsal root ganglia of STZ-induced diabetic rats alleviates tactile allodynia. Mol Med. 2015 Jun 18;21:544-52. DOI: 10.2119/molmed.2015.00063.

Towbin H, Staehelin T, Gordon J. Electrophoretic transfer of proteins from polyacrylamide gels to nitrocellulose sheets: procedure and some applications. Proc Natl Acad Sci U S A. 1979 Sep;76(9):4350-4. DOI: 10.1073/pnas.76.9.4350.

Uranga-Ocio JE, Bastús-Díez S, Delkáder-Palacios D, García-Cristóbal N, Leal-García MA, Abalo-Delgado R. Enteric neuropathy associated to diabetes mellitus. Rev Esp Enferm Dig. 2015 Jun;107(6):366-73.

Van Geldre LA, Fraeyman NH, Peeters TL, Timmermans JP, Lefebvre RA. Further characterisation of particulate neuronal nitric oxide synthase in rat small intestine. Auton Neurosci. 2004 Jan 30;110(1):8-18. DOI: 10.1016/j.autneu.2003.05.001.

Waxman SG, Kocsis JD, Black JA. Type III sodium channel mRNA is expressed in embryonic but not adult spinal sensory neurons, and is reexpressed following axotomy. J Neurophysiol. 1994 Jul;72(1):466-70. DOI: 10.1152/jn.1994.72.1.466.

Xu KY, Huso DL, Dawson TM, Bredt DS, Becker LC. Nitric oxide synthase in cardiac sarcoplasmic reticulum. Proc Natl Acad Sci U S A. 1999 Jan 19;96(2):657-62. DOI: 10.1073/pnas.96.2.657.

Yang L, Li Q, Liu X, Liu S. Roles of voltage-gated tetrodotoxin-sensitive sodium channels Nav1.3 and Nav1.7 in diabetes and painful diabetic neuropathy. Int J Mol Sci. 2016 Sep;17(9):1479-89. DOI: 10.3390/ijms17091479.

Yarandi SS, Srinivasan S. Diabetic gastrointestinal motility disorders and the role of enteric nervous system: Current status and future directions. Neurogastroenterol Motil. 2014 May;26(5):611-24. DOI: 10.1111/nmo.12330.

Zhao M, Liao D, Zhao J. Diabetes-induced mechanophysiological changes in the small intestine and colon. World J Diabetes. 2017 Jun 15;8(6):249-269. DOI: 10.4239/wjd.v8.i6.249.

Figure 1 – Glycemia and weight measurents.

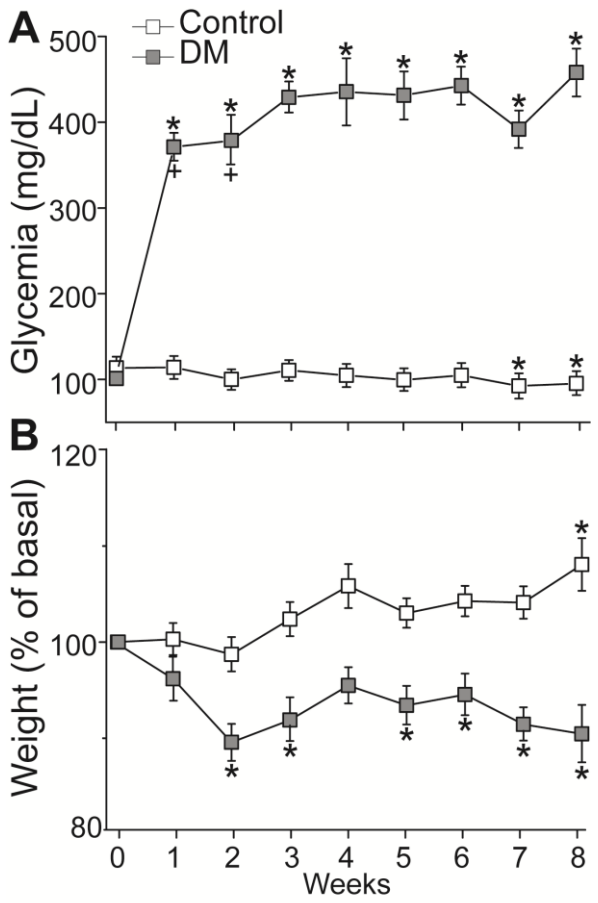

Figure 1- Hyperglycemia and weight loss in rats treated with streptozotocin. **A,** fasting blood glucose levels in rats from control or DM group, as indicated, during the course of the experiment. **B,** weight variation along the experimental time expressed as percentage change in relation to the basal weight (week 0) in rats from control or DM group. The symbol ∗ indicates statistical significance difference in control or DM rats relative to baseline measurement for glycemia (A) or weight (B). + in A indicates significant difference in relation to the last glycemic level measured in DM rats.

Figure 2 – Cholinergic efference analysis.

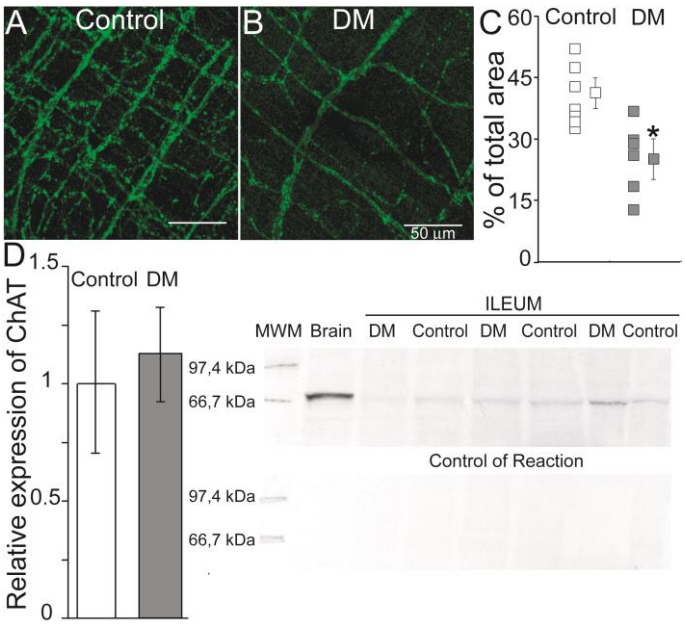

Figure 2- Thin cholinergic fiber bundles at surface of longitudinal muscle in control (**A**) and diabetes groups (**B**). **C**, analysis of density indicates a significant reduction (∗ p<0,05) in diabetes (n=6) compared to control group (n=7). Empty symbols indicate the mean data for every animal and mean ± SEM for control (n=7) group, and the filled symbols for diabetes group (n=6). **D**, western-blot analysis of ChAT expression at distal ileum. Graph represents the relative quantification of ChAT in control and diabetes group. Inset, representative western-blot experiment of homogenates from individual rats. Homogenate of brain tissue was used as positive control. The negative control of reaction, obtained when the primary antibody was omitted from reaction, is shown in the inferior panel.

Figure 3 – Neuronal density.

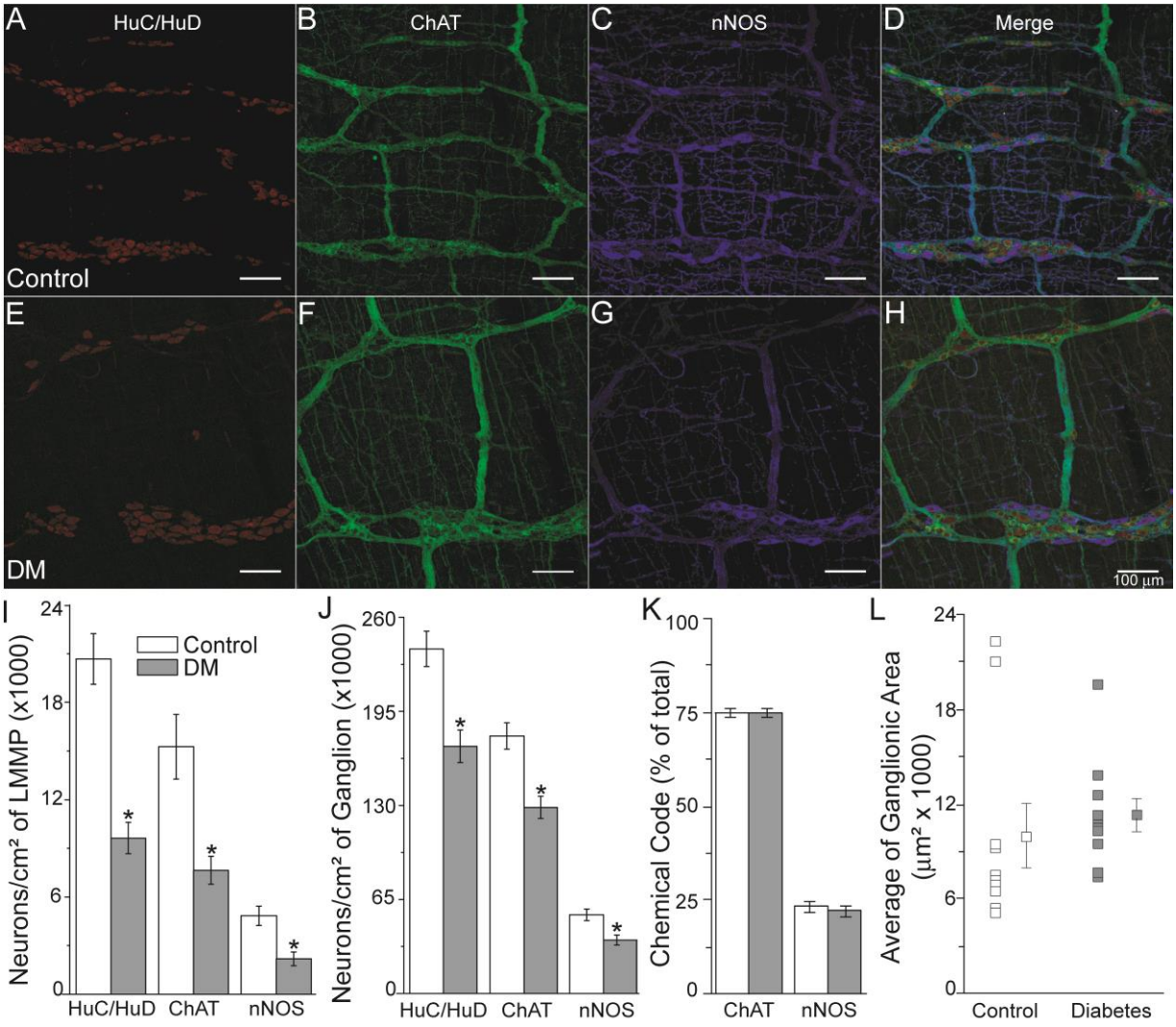

Figure 3- Triple immunofluorescence labeling of myenteric neurons from terminal ileum for HuC/HuD (**A** and **E**), ChAT (**B** and **F**), Nnos (**C** and **G**) in rats from control and diabetes groups, respectively. **D** and **H**, merge of images from control (D) and diabetes (H). **I**, Density of total (HuC/HuD positive neurons), cholinergic (ChAT positive) and nitrergic (Nnos positive) neurons in control (n=7) and diabetes (n=6 rats) groups, as indicated, expressed as number of neurons per squared centimeter of Longitudinal Muscle/Myenteric Plexus preparation (LMMP). **J**, neuronal density expressed as number of neurons per squared centimeter of ganglion area in control (n= 10) and diabetes (n= 10 rats). **K**, percentage of cholinergic and nitrergic neurons relative to total neurons in control and DM groups. **L**, mean size of myenteric ganglia measured in rats from control (□, n=10) and

diabetes groups (■, n=10). Filled circles indicate the averaged ± SEM for both groups. * indicates $p<0.05$.

Figure 4 – Antibody control.

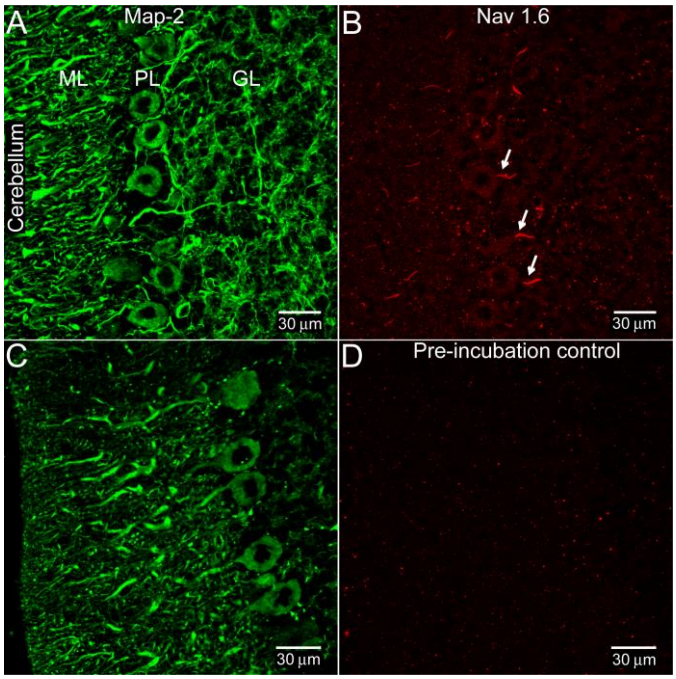

Figure 4- Anti-Nav1.6 immunolabelling at Purkinje cells from cerebellum (positive control). **A** and **C**, anti-MAP-2 labeling in soma of Purkinje cells (PL) and dendrites at molecular layer (ML) and granule cells (GL). **B**, intense anti-Nav1.6 labeling at axon initial segments (arrows) of Purkinje cells. **D**, Negative control of reaction obtained by pre-incubation of antibody with antigenic peptide.

Figure 5 – Labeling for Nav1.6.

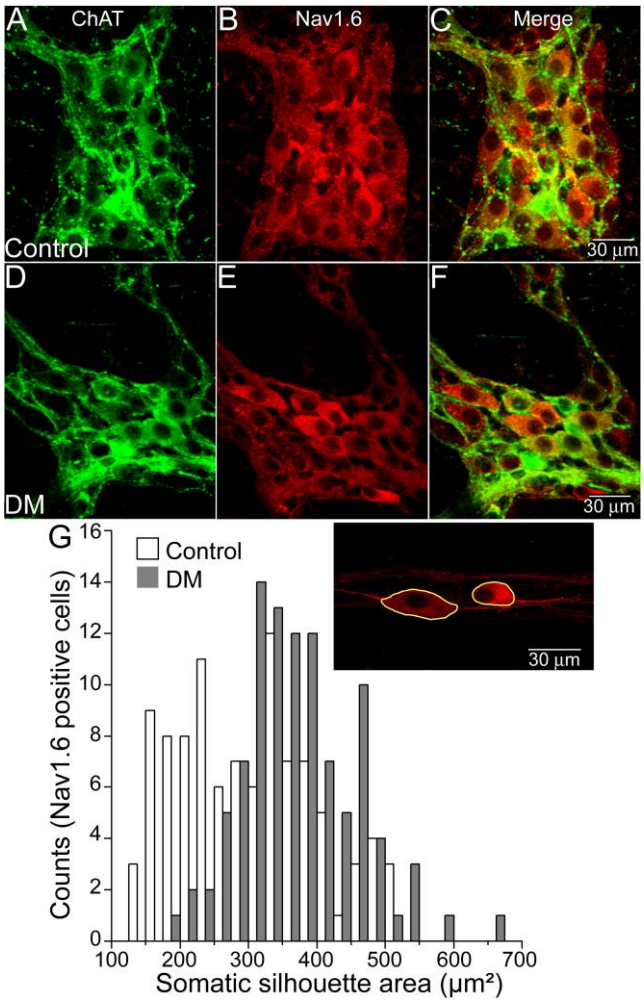

Figure 5- Double immunofluorescence labeling of myenteric neurons from terminal ileum for ChAT (**A** and **D**), Nav1.6 (**B** and **E**) and merged images (**C** and **F**) in rats from control and diabetes (DM) groups, respectively. **G**, Somatic silhouette area measured in Nav1.6 positive neurons (total of 100 cells) from both experimental groups. Inset, illustrates two Nav1.6 positive neurons with different size.

Figure 6 – RT-Qpcr experiments.

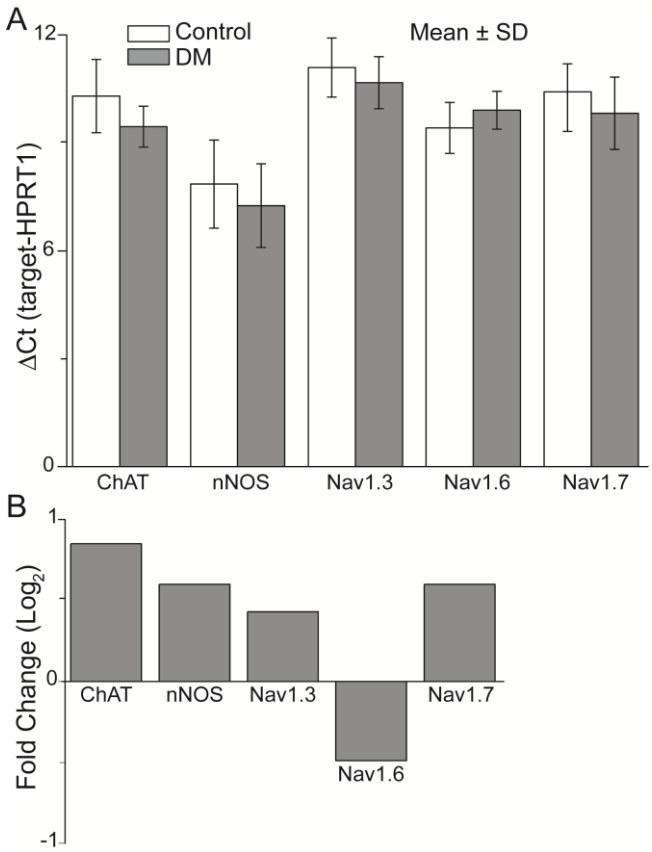

Figure 6- Relative Mrna abundance of targets genes in the control and diabetes (DM) groups. **A**, plot of mean ± SD delta Ct values in control (n=5) and diabetes (n=5) group for the different genes analyzed, as indicated. **B,** estimated fold-change for genes expression in DM group relative to control.

APÊNDICE B – Lista de participação de co-autores

Amanda Damasceno Brasileiro: Desenvolvimento do modelo experimental, experimentos de imunofluorescência, *western-blot*, aquisição de imagens, RT-qPCR, análise de dados.

Lidiane Pereira Garcia: Desenvolvimento do modelo experimental, experimentos de imunofluorescência, *western-blot*, aquisição de imagens, análise de dados.

Lenaldo Branco Rocha: Aquisição de imagens.

André Luiz Pedrosa: Experimentos de RT-qPCR.

André Shwambach Vieira: Experimentos de *western-blot* e RT-qPCR.

Valdo José Dias da Silva: Organização e delineamento experimental com os animais, análise de dados.

Aldo Rogelis Aquiles Rodrigues: Delineamento experimental geral, coordenação na execução do projeto, desenvolvimento do modelo experimental, experimentos de imunofluorescência, *western-blot*, aquisição de imagens, RT-qPCR, análise de dados.